Electron Transfer

DOI: 10.1002/ange.201208904

Electrochemical Resolution of Multiple Redox Events for Graphene Quantum Dots**

*Dhanraj B. Shinde and Vijayamohanan K. Pillai**

Metallic and semiconducting nanoclusters stabilized by a variety of organic monolayers, such as thiols, amines, and carboxylic acids, have received considerable attention in the past decade because of their size- and shape-dependent electronic, chemical, and electrochemical properties, especially because of the ease with which they show discrete single-electron transfer behavior. This intriguing behavior is specially seen as a stair case in the current–voltage behavior even at room temperature, when prepared below a critical threshold size (about 1–3 nm), having a narrow size distribution. However, the phenomenon associated with this behavior, also known as quantized double-layer (QDL) charging, has been extensively studied for some systems, using techniques such as scanning tunneling microscopy (STM), cyclic voltammetry (CV), and differential pulse voltammetry (DPV).[1–4] Some earlier reports have also demonstrated a QDL-charging behavior of clusters with larger cores (e.g. Au1400 and Au2869), where surface adsorption plays an important role in influencing the charge-storage behavior.[5] Also, much of the efforts aimed at observing the QDL charging of smaller monolayer-protected clusters (1–3 nm) have involved the use of gold particles, and there have been few reports for semiconducting quantum dots[6–10] and other metals such as Ag[11] and Pd.[12]

The discreteness of the electron charge manifests itself in the conductance as a result of the Coulomb repulsion of individual electrons. If the capacitance is a few attofarads (10^{-18} F) the charging energy turns out to be 100–150 meV, while the thermal energy is only about 26 meV. Consequently, in the presence of an external field, the system shows steps in the *I–V* characteristics because of this capacitive nature, popularly known as Coulomb blockade or single-electron transfer. Most of the reports have discussed the synthesis of smaller metal particles and their electrochemical properties, suggesting a tiny capacitor model for metal nanoclusters which show multiple peaks in voltammetric experiments, corresponding to QDL charging (single-electron transfer phenomenon in this size regime). More accurate, STM studies under high vacuum at 83 K reveal a reversible "Coulomb blockade (CB)" phenomenon, with multiple, equidistant charging steps with different bias.[1] However, no report is available on single-electron behavior either in solution phase or in solid state for GQDs (graphene quantum dots), despite its significance for applications like Field-effect transistors. Herein, we report for the first time, a clear demonstration of a discrete single-electron transfer behavior of GQDs in the 2.2 ± 0.3, 2.6 ± 0.2, and 3 ± 0.3 nm regime, where confinement of charge carriers creates an energy gap,[13] using independent experimental techniques like cyclic voltammetry and differential pulse voltammetry. A series of evenly spaced redox peaks has been observed at 273 K which corresponds to the limiting currents controlled by the diffusion of smaller particles towards the electrode surface, thus also facilitating the adsorption of GQDs.

We have recently reported an electrochemical transformation of multi-walled carbon nanotubes (MWCNTs) to GQDs by a two-step process in solution.[14] More specifically, the sustained oxidation of the MWCNTs in propylene-carbonate-containing $LiClO_4$ as supporting electrolyte at 1 V for 15 h at 90 °C is followed by reduction at −1 V for 2 h. Each step yielded discrete spherical GQD particles of tunable sizes presumably because of the lateral unzipping, in contrast to the longitudinal unzipping of CNTs to yield graphene nanoribbons.[15] As in case of most nanomaterials, even smaller variations in the size (dispersity) can exhibit a mixture of properties, that is, polydispersed samples give different potentials for the same *n*th electron and point to the importance of post-synthetic treatments for ensuring monodisperse GQDs. Hence, to obtain monodispersed GQDs (3 ± 0.3 nm), we have carried out post-synthetic size separation strategies using density gradient ultracentrifugation[16] and dialysis. These GQDs were used for further experiments after functionalization using dodecyl amine (see Figure S1 in the Supporting Information) and characterized using ultraviolet spectroscopy, photoluminescence, X-ray photoelectron spectroscopy (XPS), and Raman spectroscopy (Figures S2–S6). These GQDs are readily soluble in organic solvents, including those used here like dichloromethane (DCM). In Figure 1 a,c,e fractionation of the as-prepared GQDs after functionalization with dodecyl amine produced a larger population of monodisperse GQDs as is evident in the TEM images displaying average sizes of 3 ± 0.3, 2.6 ± 0.2, and 2.2 ± 0.3 nm, respectively. Accurate information about the change in both height and lateral dimensions, is obtained from atomic force microscopy (AFM) measurements as shown in Figure 1 b,d,f revealing a size distribution between 2.2–3 nm. However, the topographic height is between 1–2 nm indicat-

[*] D. B. Shinde
Physical and Materials Chemistry Division
National Chemical Laboratory
Pune 411 008 (India)
Prof. V. K. Pillai
Central Electrochemical Research Institute (CECRI)
Karaikudi 630 006 (India)
E-mail: vk.pillai@ncl.res.in

[**] We are grateful to Mr. Hemen and Dr. Mohammed Aslam for AFM measurements, and authors acknowledge CSIR for financial support through the project NWP0022.

Supporting information for this article is available on the WWW under http://dx.doi.org/10.1002/anie.201208904.

© 2013 Wiley-VCH Verlag GmbH & Co. KGaA, Weinheim

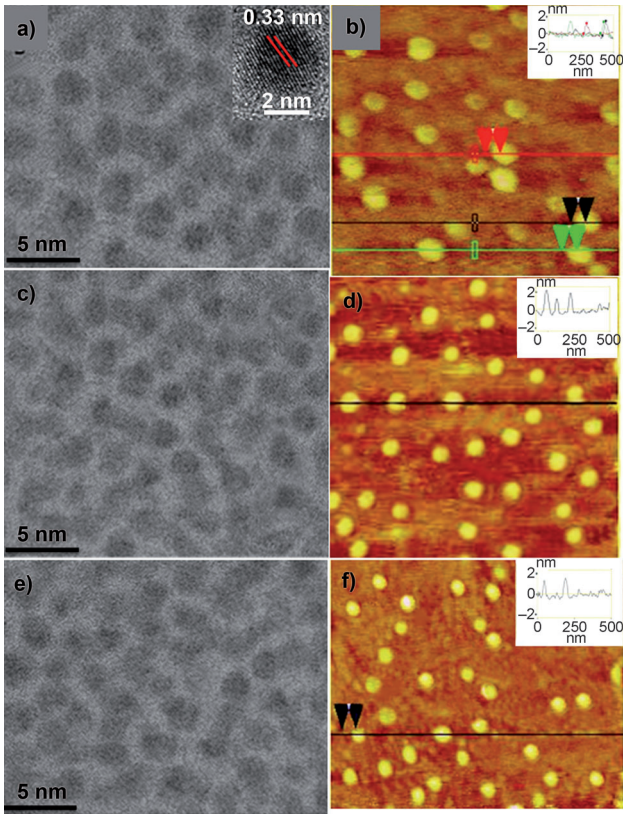

Figure 1. Typical TEM images of dodecyl-amine-capped GQDs; size and dispersion are a) 3 ± 0.3, c) 2.6 ± 0.2, and e) 2.2 ± 0.3 nm. b, d, and f) AFM images of monodisperse dodecyl-amine-capped GQDs with their corresponding height profiles displaying the presence of two to three layers of graphene in each GQDs. A clear height profile is given in Figure S7.

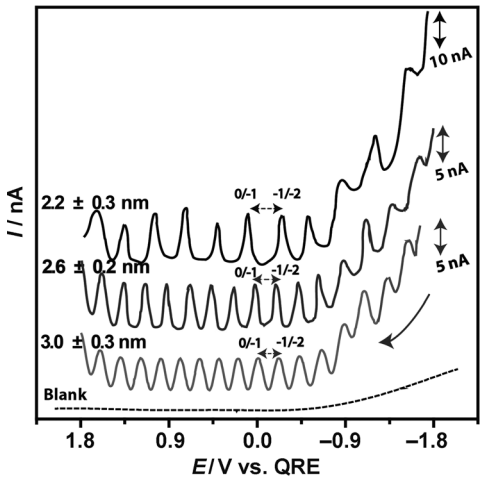

Figure 2. Differential pulse voltammetric responses of GQDs in 0.5 mM TBAHFP as supporting electrolyte in CH_2Cl_2 for particle sizes of 3 ± 0.3, 2.6 ± 0.2, and 2.2 ± 0.3 nm, using a 20 mV pulse amplitude on a Pt ultra-microelectrode (20 μm) at a typical scan rate of 25 mVs^{-1} at 273 K. A response obtained for a blank electrode (without GQDs) under similar conditions is also shown for comparison.

ing the presence of two to three layers of graphene in each individual GQD, suggesting high quality, which is also proved from the conductivity data.[14] The fact that these GQDs are much smaller than those prepared by other methods along with the strong evidence for the existence of two to three layers presumably indicates the possible origin of this single-electron transfer behavior.

A typical DPV response for the prepared GQDs revealing evenly spaced (ΔE) peaks, characteristic of charge injection to the carbon core is shown in Figure 2. After analysis of the peak spacings of the DPV data it is clear that, as the GQDs become smaller, the average distance (ΔE) between the peaks gradually increases, which suggests that ΔE is inversely proportional to the geometrical capacitance. To eliminate measurement artifacts, a blank experiment conducted without GQDs (only a Pt ultra-microelectrode with all other identical parameters) is also shown in the same plot for comparison as artifacts cannot provide these single-electron transfer peaks with uniform width, whereas the peak potential varies with the charge number consistently as given in the Nernst equation. The peak potentials can be taken as the formal redox potential $E^{\circ\prime}$ for the redox couple of each GQDs with a $z/z\pm1$ charge number since GQDs were presumed to be formed by reduction at -1 V, which helps to assign a charge of $z=-1$. Accordingly, the first two peaks (oxidation and reduction peaks adjacent to E_{pzc}) could correspond to the 0/-1 and $-1/-2$ redox couple, respectively. The charge steps are marked in the graph for comparison with respect to the Pt quasi-reference electrode assuming the potential of zero charge as the minima of the blank electrode under similar conditions. Interestingly, the full-width at half-maximum (FWHM) of each peak is found to be about 90 mV, which is comparable to earlier reports of smaller-sized Au Q-dots (82 mV at 273 K).[17,18] This small variation in the FWHM might be attributed to several complex interactions of these charged GQDs in the vicinity of the electrode surface. For example, these GQDs can be viewed as an assembly of mixed valent redox centers at the electrode–solution interfaces during electrochemical processes. There are also possibilities for the reorganization of charges among the GQDs by electron self-exchange or disproportionation. The FWHM of differently sized GQDs is identical to the expected value in case of single-electron transfer in semiconductor Q-dots.[19] These regularly spaced peaks are sharp, reversible, highly reproducible, and comparable to similar single-electron transfer processes of Si[8] and CdTe[10] Q-dots. This is the first report of such a remarkable resolution of individual redox peaks for GQDs at 273 K which undoubtedly confirms that GQDs are indeed multivalent species.

Figure 3a represents the "Z plot" for GQDs corresponding to the DPV response as shown in Figure 2, where linear ($R^2>0.99$) behavior can be seen as expected for the ideal QDL behavior.[17,20] The C_{GQD}, and corresponding charging energy values calculated from the slope of the "Z plot" are given in Table 1. The variation of the peak spacing (ΔE) with the charge number $z/z-1$ reveals that the voltage spacing is extremely regular for GQDs at a positive potential despite a minor irregularity at the negative potential end; possibly because of impurities or solvent decomposition.[21] Also, the gap between the onset of oxidation and reduction, that is, the HOMO–LUMO gap, estimated for these GQDs as found

© 2013 Wiley-VCH Verlag GmbH & Co. KGaA, Weinheim

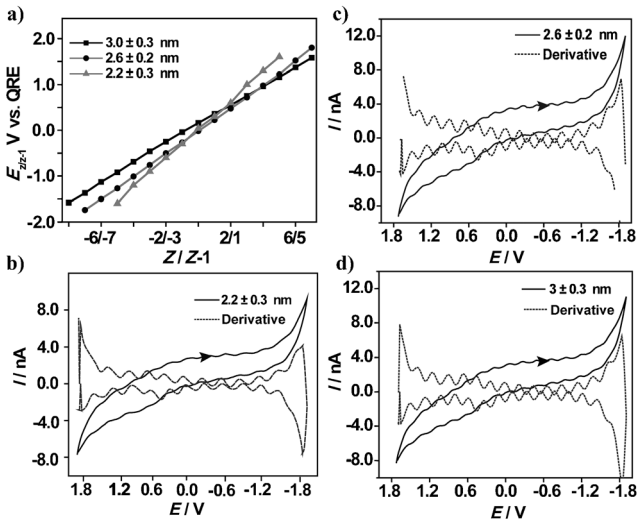

Figure 3. a) Plot of $E^{0\prime}$ vs. the redox couple charge ($z/z\pm1$) for GQDs of different sizes, where linear ($R^2>0.99$) behavior can be seen as expected for the ideal QDL behavior using the Nernst equation. Superimposed cyclic voltammetric response of the GQDs of b) 2.2 ± 0.3, c) 2.6 ± 0.2, and d) 3 ± 0.3 nm at 100 mVs^{-1} in DCM with 0.5 mM TBAHFP on a Pt ultra-microelectrode, with its derivative response showing a series of QDL charging steps.

Table 1: The relative variation in the capacitance, HOMO–LUMO gap, and charging energy for differently sized GQDs.

Size of the GQDs [nm]	Capacitance [aF]	HOMO–LUMO gap [eV]	Charging energy [meV]
2.2 ± 0.3	0.50	0.36	151
2.6 ± 0.2	0.63	0.25	125
3.0 ± 0.3	0.76	0.21	104

from the DPV plot is inversely varying with size, which is in good agreement with similar trends in case of GQDs and graphene nanoribbons[13,22–27] notwithstanding the difference in morphology.

The quantized double layer (QDL) charging of the GQD core occurs because the effective capacitance (C_{GQD}) with a core diameter <3 nm is so small (sub-attofarads) that a single-electron change to their core charges occurs at large voltage intervals. These capacitance values are comparable to that of semiconducting QDs having sizes of 4–5 nm. The charging energy E_c of the GQDs is calculated using Equation (1),

$$E_c = \frac{e^2}{2C_{GQDs}} \quad (1)$$

which is in excellent agreement with criteria for the single-electron charging $E_c \geq kT$ (where k is the Boltzmann constant) at 273 K.[17] Otherwise, thermally activated electrons will overcome the Coulomb barrier and escape from the GQDs.

In comparison to the DPV analysis, CV resolves this remarkably high population of charge steps, where the derivative response is particularly comparable with DPV results. CV and DPV show consecutive n electrochemical reactions for the GQDs, each by transfer of a new electron giving a new ionic compound. Indeed the type of doping, either p-doping (extraction of electrons from the GQD) or n-doping (injection of electrons to the GQD), is implicit in both the DPV and CV results, in which the potential of zero charge separates these regions. Similar processes are followed by fullerenes, carbon nanotubes, or conducting polymers and estimation of the HOMO–LUMO gap is based on this concept. Figure 3 b–d shows the cyclic voltammetric response of the GQDs of different sizes at a 100 mVs^{-1} scan rate superimposed with its derivative response. Since GQDs act as tiny capacitors (with a charge storage capability of the order of attofarads, that is, 10^{-18} F) the peak-to-peak spacing of the derivate of the CV shows close similarity, with the corresponding peaks seen in the DPV. These ΔE values are also invariant with pulse width (40 mV) as shown in Figure S8. Similar DPV results for GQDs of larger size (>5 nm) interestingly do not show a single-electron transfer behavior at 273 K since Equation (1) cannot be obeyed presumably because of higher capacitance values. Thus a combined analysis of the experimental data from DPV, CV, AFM, and TEM clearly reveals that dodecyl-amine-capped GQDs act as multivalent redox species, revealing evenly spaced (ΔE) peaks because of charge injection to the semiconducting core. The origin of small irregularity in peak spacing at negative potential needs to be investigated further by considering other possible sources like solvent decomposition. Further experiments using different solvent and supporting electrolyte combinedly reveal the exact origin of this anomalous behavior in the negative potential. Also, temperature-dependent single-electron transfer behavior of these differently sized GQDs is under investigation in our lab.

In conclusion, we show that GQDs of tunable sizes of 2.2 ± 0.3, 2.6 ± 0.2, and 3 ± 0.3 nm can act as multivalent redox species using various electrochemical techniques, such as CV and DPV measurements, and present exciting opportunities for a variety of applications including single-electron transistors, molecular switches, and resonant tunneling diodes; because of attofarad charge storage and the number of electron-transfer events. It is also useful for biomimetic applications like artificial muscles, batteries, smart membranes, and smart drug-delivery devices.[28] The capacitance values calculated from the experimental data (in the range of attofarads) are in good agreement with a single-electron transfer phenomenon at 273 K. While the TEM images display both the tunable size and monodisperse nature of the GQDs, AFM measurements offer indirect evidence for the presence of two to three graphene-like layers for the smallest GQDs. The physical and electrochemical properties of these ultrasmall GQDs could provide interesting opportunities for the use of these size-tunable narrow band gap semiconductors as future materials for nanoelectronic devices.

Experimental Section

The graphene quantum dots were synthesized according to our previous work.[14] The GQDs having carboxyl groups were useful sites

© 2013 Wiley-VCH Verlag GmbH & Co. KGaA, Weinheim

for further modifications, as they enable the covalent coupling of molecules through the creation of amide bonds (Figure S1). In Figure 1 a,c,e fractionation of as-prepared GQDs after functionalization with dodecyl amine has produced a larger population of monodisperse GQDs, which is evident in the TEM images displaying average sizes (3 ± 0.3, 2.6 ± 0.2, and 2.2 ± 0.3 nm), respectively. The samples for FTIR measurements were prepared by grinding the GQDs into potassium bromide at a concentration of about 0.03 wt%. The GQDs show a broad peak at about 3450 cm^{-1}, which refers to the O–H stretch of the hydroxyl group (Figure S3), which can be ascribed to the oscillation of carboxyl groups. A small peak at 1708 cm^{-1} is associated with the stretch mode of carboxylic groups as observed for GQDs, carboxylic groups are formed because of the oxidation of some carbon atoms on the surface of the GQDs. New peaks appeared after dodecyl amine treatment at 1123 and 3500–3700 cm^{-1}, respectively, and can be assigned to C–N in-plane, and N–H in-plane stretching of the amide groups.[29] A characteristic amide–carbonyl (-NH-CO) stretching vibration was observed at 1624 cm^{-1}, which implies the formation of amide groups through interactions with -COOH.[30] The peak at 1448 cm^{-1} is attributed to the overlapping of a signal from the N–H bending mode of vibrations. All electrochemical measurements were carried out by using the dodecyl-amine-capped GQDs after purification by dialysis and density gradient ultracentrifugation. Subsequently, the GQDs (2 mg) were dissolved in dichloromethane (10 mL) and all voltammetric experiments were carried out using a Pt ultra-microelectrode (UME, 20 μm) as working electrode, a Pt foil as counter electrode, and a Pt wire as a reference electrode using a conventional system which is calibrated prior to all experiments against the ferrocene–ferrocenium couple. DPV responses of the GQDs were recorded using 0.5 mM tetra(*n*-butyl)ammonium hexafluorophosphate (TBAHFP) as supporting electrolyte in CH_2Cl_2 for particle sizes of 3 ± 0.3, 2.6 ± 0.2, and 2.2 ± 0.3 nm, using a 20 mV pulse amplitude at a typical scan rate of 25 $mV\,s^{-1}$.

Received: November 7, 2012
Revised: December 19, 2012
Published online: January 29, 2013

Keywords: charging energy · differential pulse voltammetry · graphene · quantum dots · single-electron transfer

[1] R. S. Ingram, M. J. Hostetler, R. W. Murray, T. G. Schaaff, J. Khoury, R. L. Whetten, T. P. Bigioni, D. K. Guthrie, P. N. First, *J. Am. Chem. Soc.* **1997**, *119*, 9279.
[2] S. Chen, R. S. Ingram, M. J. Hostetler, J. J. Pietron, R. W. Murray, T. G. Schaaff, J. T. Khoury, M. M. Alvarez, R. L. Whetten, *Science* **1998**, *280*, 2098.
[3] A. C. Templeton, W. P. Wuelfing, R. W. Murray, *Acc. Chem. Res.* **2000**, *33*, 27.
[4] S. J. Chen, *Electroanal. Chem.* **2004**, *574*, 153.
[5] N. K. Chaki, P. Singh, C. V. Dharmdhikari, V. K. Pillai, *Langmuir* **2004**, *20*, 10208.
[6] P. Hoyer, H. Weller, *Chem. Phys. Lett.* **1994**, *221*, 379.
[7] S. Chen, L. A. Truax, J. M. Sommers, *Chem. Mater.* **2000**, *12*, 3864.
[8] Z. Ding, B. M. Quinn, S. K. Haram, L. E. Pell, B. A. Korgel, A. J. Bard, *Science* **2002**, *296*, 1293.
[9] S. K. Haram, B. M. Quinn, A. J. Bard, *J. Am. Chem. Soc.* **2001**, *123*, 8860.
[10] Y. Bae, Y. Myung, A. J. Bard, *Nano. Lett.* **2004**, *4*, 1153.
[11] W. Cheng, S. Dong, E. Wang, *Electrochem. Commun.* **2002**, *4*, 412.
[12] S. Chen, K. Huang, J. A. Stearns, *Chem. Mater.* **2000**, *12*, 540.
[13] a) A. K. Geim, K. S. Novoselov, *Nat. Mater.* **2007**, *6*, 183; b) M. Y. Han, B. O. Zyilmaz, Y. Zhang, P. Kim, *Phys. Rev. Lett.* **2007**, *98*, 206805; c) F. Sols, F. Guinea, A. H. C. Neto, *Phys. Rev. Lett.* **2007**, *99*, 166803; d) F. Miao, F. Miao, S. Wijeratne, Y. Zhang, U. C. Coskun, W. Bao, C. N. Lau, *Science* **2007**, *317*, 1530; e) C. Stampfer, J. Guttinger, F. Molitor, D. Graf, T. Ihn, K. Ensslin, *Appl. Phys. Lett.* **2008**, *92*, 012102; f) J. S. Bunch, Y. Yaish, M. Brink, K. Bolotin, P. L. McEuen, *Nano Lett.* **2005**, *5*, 287.
[14] D. B. Shinde, V. K. Pillai, *Chem. Eur. J.* **2012**, *18*, 12522.
[15] D. B. Shinde, J. Debgupta, A. Kushwaha, M. V. Aslam, V. K. Pillai, *J. Am. Chem. Soc.* **2011**, *133*, 4168.
[16] L. M. Melanie, M. F. Florian, F. Daniel, J. H. Eric, K. Christian, L. Uli, A. O. Geoffrey, *Nano Lett.* **2012**, *12*, 337.
[17] D. T. Miles, R. S. Murray, *Anal. Chem.* **2003**, *75*, 1251.
[18] R. W. Murray, *Chem. Rev.* **2008**, *108*, 2688.
[19] J. D. Holmes, K. J. Ziegler, R. C. Doty, L. E. Pell, K. P. Johnston, B. A. Korgel, *J. Am. Chem. Soc.* **2001**, *123*, 3743.
[20] S. J. Green, J. J. Stokes, M. J. Hostetler, J. Pietron, R. W. Murray, *J. Phys. Chem. B* **1997**, *101*, 2663.
[21] B. M. Quinn, P. Liljeroth, V. Ruiz, T. Laaksonen, K. Kontturi, *J. Am. Chem. Soc.* **2003**, *125*, 6644.
[22] H. Raza, E. C. Kan, *Phys. Rev. B* **2008**, *77*, 245434.
[23] Y. W. Son, M. L. Cohen, S. G. Louie, *Phys. Rev. Lett.* **2006**, *97*, 216803.
[24] V. Barone, O. Hod, G. E. Scuseria, *Nano Lett.* **2006**, *6*, 2748.
[25] M. Y. Han, B. Ozyilmaz, Y. B. Zhang, P. Kim, *Phys. Rev. Lett.* **2007**, *98*, 206805.
[26] Z. H. Chen, Y. M. Lin, M. J. Rooks, P. Avouris, *Physica E* **2007**, *40*, 228.
[27] X. L. Li, X. R. Wang, L. Zhang, S. W. Lee, H. J. Dai, *Science* **2008**, *319*, 1229.
[28] J. G. Martinez, T. F. Oteroa, C. B. Navarro, E. Coronado, C. M. Gastaldo, H. P. Garcia, *Electrochim. Acta* **2012**, *81*, 49.
[29] Y. P. Sun, W. Huang, Y. Lin, K. Fu, A. Kitaygorodskiy, L. A. Riddle, Y. J. Yu, D. L. Carroll, *Chem. Mater.* **2001**, *13*, 2864.
[30] K. Fu, W. Huang, Y. Lin, L. A. Riddle, D. L. Carroll, Y. P. Sun, *Nano Lett.* **2001**, *1*, 439.

 © 2013 Wiley-VCH Verlag GmbH & Co. KGaA, Weinheim